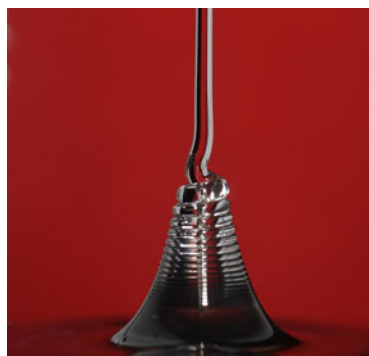


A sticky situation

P.-T. Brun[†]

Department of Mathematics, Massachusetts Institute of Technology, Cambridge, MA 02139, USA



The whirling helical structure obtained when pouring honey onto toast may seem like an easy enough problem to solve at breakfast. Specifically, one would hope that a quick back-of-the-envelope scaling argument would help rationalize the observed behaviour and predict the coiling frequency. Not quite: multiple forces come into play, both in the part of the flow stretched by gravity and in the coil itself, which buckles and bends like a rope. In fact, the resulting abundance of regimes requires the careful numerical continuation method reported by Ribe (*J. Fluid Mech.*, vol. 812, 2017, R2) to build a complete phase diagram of the problem and untangle this sticky situation.

Key words: instability, interfacial flows (free surface), nonlinear dynamical systems

1. Introduction

Consider the breakfast table experiment that consists in pouring honey, syrup or any sufficiently viscous liquid onto a piece of toast or a stack of pancakes. While its mundane nature would suggest that the behaviour should be easily predictable, the liquid rope-coil effect displayed by such a drizzling thread is a sticky situation that has long resisted the onslaughts of theoreticians aiming to elucidate its intricate dynamics. This anomaly may be even more of a surprise to fluid dynamicists, who would anticipate that the low dimensionality of the problem – a thread is essentially a one-dimensional object defined along its centreline – would facilitate its theoretical treatment. Perhaps such theoretical difficulties are best illustrated by noting that this type of flow behaves like an elastic medium rather than a conventional free-surface flow. In particular, the stream maintains its topological integrity throughout the entire dynamics, and does not immediately spread on the substrate upon impact – by contrast with an axisymmetric stagnation flow – but instead buckles into a helical structure similar to that observed when a mountaineer's rope falls on the ground. As a consequence, the classical toolbox of fluid mechanics, such as linear stability analysis or – at the other end of the spectrum – numerical methods such as the volume-of-fluid approach, are not easily applicable to this problem. Instead, viscous

[†] Email address for correspondence: ptbrun@mit.edu

The figure by the title reproduced by kind permission of H. Hosseini.

rods are more amenable to a dimensionally reduced version of the Navier–Stokes equations, which takes the form of the Kirchhoff equations for elastic rods, and which accounts for the dynamics of the thread’s centreline endowed with finite resistance to stretching, bending and twisting (Ribe 2004; Ribe *et al.* 2006; Brun, Ribe & Audoly 2012; Audoly *et al.* 2013). Additionally, this problem is made more tractable by taking advantage of two key features: coiling is a steady problem when viewed in the co-rotating reference frame and surface tension is not essential to the problem and thus may be neglected.

Because viscous threads occur frequently in nature and in a broad range of engineering processes, liquid rope coiling and related problems have been studied extensively using experimental, theoretical and numerical approaches. While traditional applications include non-woven textile production, it has recently been shown that coiling instabilities may be controlled and harnessed to create new fabrication pathways in ‘3D printing’. Despite significant progress in recent years in identifying the different modes of coiling depending on the relative magnitudes of viscous stresses, gravity and inertia (see Ribe *et al.* (2012) for a review), a complete regime diagram as a function of the control parameters of the problem was lacking.

2. Overview

Along a freely falling stream of liquid, the gravity-induced stretching of the thread is resisted by viscous forces and inertia, yielding a typical length scale, $L^* = (\nu^2/g)^{1/3}$, and time scale, $T^* = (\nu/g^2)^{1/3}$. Here, ν is the fluid viscosity and g the acceleration of gravity. For heights of fall $H < L^*$, viscous stresses balance gravity, whereas inertia dominates the dynamics for larger values of H . In the coiling problem defined in figure 1(a), the flow naturally divides into two parts. In the upper part or tail, the thread is mostly accelerated vertically and deformation is solely by stretching. At the lowest point of the tail, the thread of radius a_1 connects to a boundary layer that buckles and coils. Scaling arguments may be used to estimate the arcwise extent of this region, $\delta^* = (\nu Q/g)^{1/4}$, where Q is the flow rate imposed at the nozzle with diameter d . In the coil, the thread’s radius is nearly constant and the thread mostly deforms by bending and twisting so as to accommodate the no-slip boundary condition on the substrate. Specifically, the flow speed in the coil derived from mass conservation, $U_c = Q/(\pi a_1^2)$, imposes the speed of coiling given by the product $R\Omega$, where R is the coiling radius and Ω the coiling frequency.

Dimensional analysis applied to the problem, neglecting capillary effects, reveals the existence of four independent dimensionless groups. The dimensionless coiling frequency $\Pi_\Omega = \Omega T^*$ is thus a function of the dimensionless height of fall $\Pi_H = H/L^*$, the dimensionless flow rate $\Pi_Q = QT^*/L^{*3}$ and the dimensionless nozzle diameter $\Pi_d = d/\delta^*$. Ribe (2017) proposes a complete phase diagram of the problem in the form of contour plots of Π_Ω as a function of Π_H , Π_Q and Π_d , an example of which is provided in figure 1(c). A natural starting point of this approach is the investigation of the existence of coiling solutions in the (Π_H, Π_Q, Π_d) phase space. To this end, Ribe (2017) uses a self-intersection geometric criteria: coiling is possible only if the thread’s radius in the coil, a_1 , is less than the radius of coiling R , otherwise, the rope would self-intersect. The implementation of this condition builds on the numerical algorithm of Ribe (2004), here used to determine $a_1(\Pi_H, \Pi_Q, \Pi_d)$ and $R(\Pi_H, \Pi_Q, \Pi_d)$. In practice, for a given value of Π_d , a valid coiling solution with $a_1 < R$ is used as starting point, and parameters are changed in the (Π_H, Π_Q) space until the condition $a_1 = R$ is met. Such a limit solution is then continued so as to draw the curve in the

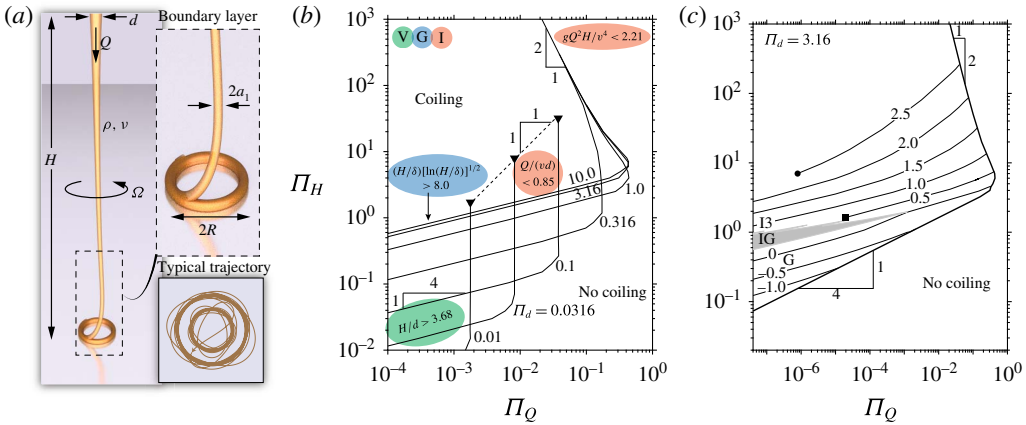


FIGURE 1. (a) Statement of the problem: the thread comprises a tail and a coil. Inset: a typical trajectory of the contact point between the thread and the substrate obtained while varying H . (b) Contours of $a_1 = R$ in the (Π_H, Π_Q) space for several values of Π_d . They separate regions where coiling solutions exist from regions where they do not exist. (c) Complete phase diagram showing iso-contours of Π_Ω in the (Π_H, Π_Q) space for a value of Π_d (adapted from Ribe (2017)).

plane that separates regions where coiling solutions exist from regions where they do not exist (figure 1b).

These results can be examined in light of the mechanics at play in the coil. Specifically, the viscous forces that resist bending in this boundary layer may act alone (defining the viscous regime V), or be balanced by gravity (regime G), inertia (regime I) or a combination of both (regime IG, where Π_Ω is multivalued). These regimes appear in the order V/G/IG/I as the fall height increases. Despite the wealth of regimes, Ribe (2017) obtains remarkably simple expressions for the boundaries of the domain of existence of steady coiling solutions. They are reported in figure 1(b) and are colour-coded according to the regime from which they are derived. Within the domain of existence of coiling, the same numerical method may be used to map the iso-contours of Π_Ω (or equivalently the radius of coiling). For the regimes V, G and I, Π_Ω is single valued (see the plots in figure 1(c) obtained for a representative value of Π_d). However, in the regime IG Π_Ω is multivalued, giving rise to sudden transitions in Ω (and R) and hysteresis as multiple coiling solutions are in competition. In figure 1(a), the radius of coiling is shown to suddenly increase dramatically as H is decreased. This transition corresponds to a fold in the coiling solution such that the system jumps from one solution branch to another. This regime originates from the coupling between the thread’s whirling modes and the inner machinery of the coil. The IG regimes are represented by shaded areas in the diagram, owing to the multivaluedness of the function in these regions. Nevertheless, the value(s) of Π_Ω is known at any point of the (Π_H, Π_Q) plane so that these diagrams fully characterize the coiling frequency for given values of the control parameters of the problem: fall height, flow rate, viscosity and nozzle diameter.

3. Future

With the complete phase diagram for the coiling frequency and expressions for its boundaries and iso-contours, it appears that the dynamics of a thread impacting a flat

substrate is very well understood. In particular, this base of knowledge is of practical interest in the context of engineering applications. Future work will consist in building on these theoretical results to devise design guidelines in ‘extreme’ environments, i.e. where traditional fabrication techniques fail and alternative instability-mediated routes are needed or preferable.

While this point is valid, viscous threads have not yet yielded up all their secrets. A direct continuation of the work of Ribe (2017) consists in pushing further the analysis of the interplay between tail and coil in the IG regime. In this regime, the fold points of the $\Pi_{\Omega}(\Pi_H)$ coiling solutions match the thread’s resonant modes in virtue of their coupling with the coil’s dynamics. This interplay is directly relevant to the fluid mechanical sewing machine, i.e. a thread falling onto a conveyor belt – a direct analogue of 3D printing (see Chiu-Webster & Lister 2006). In this case, the cylindrical symmetry of coiling is broken by the belt so that non-trivial steady solutions are impossible, giving rise to a variety of ‘stitching’ patterns. Past work has shown the immediate applicability of steady coiling results to rationalizing the formation of such patterns. Specifically, Brun *et al.* (2015) have shown that the coiling speed is the relevant scale to compare to the belt’s speed and that the trajectory of the thread’s contact point with the belt is analogous to steady coiling, both in terms of radius of curvature and Fourier spectrum (these quantities are related to $1/R$ and Ω , respectively). In the IG regime, these quantities are multivalued, so that the results of Brun *et al.* (2015) are not directly applicable. This point is all the more fascinating, since complex patterns, possibly chaotic, are observed. Further insight into the delicate coupling between tail and coil would help reveal the blueprint of such patterns.

Returning to steady coiling, a crucial approximation is made in the work of Ribe (2017): that the thread immediately stops when it makes contact with the substrate (no-slip boundary condition). This boundary condition is central to the problem, as it is the one creating the deceleration that yields buckling. While it is in general the best condition to impose, it does not always fully represent the physical problem. Indeed, the thread can either build up a corkscrew-like structure, whose size varies over time, or else spread after impact, sometimes generating propagating spiral waves of air bubbles. Such behaviours cannot be directly modelled with the present method, and their treatment would require some coupling with a more traditional fluid mechanics solver (such as direct numerical simulation) or a lubrication-like approach. This observation completes our initial statement on the theoretical difficulties in modelling coiling. Liquid threads behave like rods for the most part, yet in the end their fluidic nature prevails: a sticky situation.

References

- AUDOLY, B., CLAUVELIN, N., BRUN, P.-T., BERGOU, M., GRINSPUN, E. & WARDETZKY, M. 2013 A discrete geometric approach for simulating the dynamics of thin viscous threads. *J. Comput. Phys.* **253**, 18–49.
- BRUN, P.-T., AUDOLY, B., RIBE, N. M., EAVES, T. S. & LISTER, J. R. 2015 Liquid ropes. *Phys. Rev. Lett.* **114** (17), 174501.
- BRUN, P.-T., RIBE, N. M. & AUDOLY, B. 2012 A numerical investigation of the fluid mechanical sewing machine. *Phys. Fluids* **24** (4), 043102.
- CHIU-WEBSTER, S. & LISTER, J. R. 2006 The fall of a viscous thread onto a moving surface: a fluid-mechanical sewing machine. *J. Fluid Mech.* **569**, 89–111.
- RIBE, N. M. 2004 Coiling of viscous jets. *Proc. R. Soc. Lond. A* **460**, 3223–3239.
- RIBE, N. M. 2017 Liquid rope coiling: a synoptic view. *J. Fluid Mech.* **812**, R2.
- RIBE, N. M., HABIBI, M. & BONN, D. 2012 Liquid rope coiling. *Annu. Rev. Fluid Mech.* **44**, 249–266.
- RIBE, N. M., HUPPERT, H. E., HALLWORTH, M. A., HABIBI, M. & BONN, D. 2006 Multiple coexisting states of liquid rope coiling. *J. Fluid Mech.* **555**, 275–297.